



Published in final edited form as:

*Alzheimers Dement.* 2021 February ; 17(2): 149–163. doi:10.1002/alz.12256.

## Reactive or transgenic increase in microglial TYROBP reveals a TREM2-independent TYROBP-APOE link in wild-type and Alzheimer's-related mice

Mickael Audrain<sup>1</sup>, Jean-Vianney Haure-Mirande<sup>1</sup>, Justyna Mleczko<sup>1</sup>, Minghui Wang<sup>2</sup>, Jennifer K. Griffin<sup>3</sup>, Peter H. St George-Hyslop<sup>3</sup>, Paul Fraser<sup>3</sup>, Bin Zhang<sup>2</sup>, Sam Gandy<sup>1,4,5,\*</sup>, Michelle E. Ehrlich<sup>1,2</sup>

<sup>1</sup>Department of Neurology, Icahn School of Medicine at Mount Sinai, New York, NY 10029, USA

<sup>2</sup>Department of Genetics and Genomic Sciences and Icahn Institute of Genomic Sciences, Icahn School of Medicine at Mount Sinai, New York, NY 10029, USA

<sup>3</sup>Tanz Centre for Research in Neurodegenerative Diseases, University of Toronto, Toronto, ON. M5T OS8, Canada

<sup>4</sup>National Institute on Aging-Designated Alzheimer's Disease Research Center and Department of Psychiatry, Icahn School of Medicine at Mount Sinai, New York, NY 10029, USA

<sup>5</sup>Research and Development, James J. Peters Veterans Affairs Medical Center, Bronx, NY 10468, USA

### Abstract

**Introduction**—Microglial TYROBP (DAP12) is a network hub and driver in sporadic late-onset Alzheimer's disease (AD). TYROBP is a cytoplasmic adaptor for TREM2 and other receptors, but little is known about its roles and actions in AD. Herein, we demonstrate that endogenous *Tyrobp* transcription is specifically increased in recruited microglia.

**Methods and Results**—Using a novel transgenic mouse overexpressing TYROBP in microglia, we observed a decrease of the amyloid burden and an increase of TAU phosphorylation stoichiometry when crossed with *APP/PSEN1* or *MAPT<sup>P301S</sup>* mice, respectively. Characterization of these mice revealed *Tyrobp*-related modulation of *ApoE* transcription. We also showed that *Tyrobp* and *ApoE* mRNAs were increased in *Trem2*-null microglia recruited around either A $\beta$  deposits or a cortical stab injury. Conversely, microglial *ApoE* transcription was dramatically diminished when *Tyrobp* was absent.

\*Correspondence: samuel.gandy@mssm.edu.

#### AUTHOR CONTRIBUTIONS

MA, JVHM, SG and MEE designed the study. MA performed the experiments and analyzed the data. JM contributed to the RNA *in situ* hybridization related experiments. MW and BZ contributed to the RNA sequencing analysis. JKG, PHStGH and PF provided the *TgCRND8* mice. MA, SG and MEE wrote the manuscript.

#### CONFLICT OF INTEREST

The authors declare that they have no competing interests.

**Conclusions**—Our results provide evidence that TYROBP-APOE signaling does not require TREM2 and could be an initiating step in establishment of the Disease-Associated Microglia (DAM) phenotype.

### Keywords

Tyrobp; Dap12; Apoe; Trem2; microglia; Alzheimer's disease; amyloid; APP/PSEN1; tauopathy; PS19; RNAscope; DAM

## 1. NARRATIVE

### 1.1 Contextual background

Microglia play a sentinel role in the brain, capable of detecting a wide variety of environmental stimuli, including microbial pathogens, aggregated proteins (such as amyloid- $\beta$ ; A $\beta$ ) and cellular debris (such as membrane fragments). This sensing activity is an essential part of the host response and is broad in its scope, sometimes triggering homeostatic adjustment, while, at other times, activating a host defense response. Microglia are also of interest in neurodegenerative diseases due to proteinopathies, e.g. Alzheimer's disease (AD), in which large genetic studies have reported increased disease risk linked to many loci associated with microglial genes implicated in clearance of A $\beta$  peptides[1–9]. More recently, transcriptomic analyses have revealed distinct profiles and signatures for microglia associated with aging and aging-related diseases, indicating that a wide range of specific proteins in microglia underlies sensing, activation, and/or other cellular responses. Using RNA sequencing, Hickman et al. (2013) identified 100 transcripts highly enriched in microglia and coined the term “sosome” to describe this class of microglial transcripts[10]. Network analysis of this list identified a *TYROBP* (for tyrosine kinase binding protein; also known as *DAP12*, for DNAX activating protein-12)-centered pathway with 24 of these 100 genes interacting directly with *TYROBP* and 20 interacting indirectly with *TYROBP*. Concurrently, members of our team employed an integrative network-based approach and identified *TYROBP* as a key network driver in sporadic late-onset Alzheimer's disease (AD) [11]. More recently, Keren-Shaul *et al.*[12] used single-cell RNA sequencing in mouse to define a specific microglial phenotype that they termed “Disease-Associated Microglia” (DAM). *Tyrobp* was one of the genes most robustly upregulated in the proposed earliest stage of transition of microglia from the basal “homeostatic state” into the DAM phenotype.

*TYROBP* is a transmembrane signaling polypeptide that contains an immunoreceptor phosphotyrosine-based activation motif (ITAM) in its cytoplasmic domain. *TYROBP* is expressed in microglia in the brain and serves as an adaptor for a variety of immune receptors, including two molecules closely linked to AD pathogenesis: TREM2 (triggering receptor expressed on myeloid cells 2) and CR3 (complement receptor 3). TREM2 is expressed at the plasma membrane of microglia in the brain and some mutations and polymorphisms of *TREM2* are linked to autosomal dominant AD or sporadic late-onset AD[13]. Other *TREM2* mutations can cause a polycystic leukoencephalopathy osteodystrophy also known by the eponym Nasu-Hakola disease[14]. Most *TYROBP* mutations represent loss-of-function mutations and also result in Nasu-Hakola disease[15]. Similarly, *TYROBP* genetic variants have been identified in early-onset AD[16]. TREM2 is

(among other things) a microglial A $\beta$  receptor promoting microglial phagocytosis and proliferation and is required in order for microglia to limit growth of A $\beta$  deposits[17,18]. In addition to the influences of environmental factors on TREM2[19], this molecule is also essential for a full transition of homeostatic microglia to a DAM state. Keren-Shaul *et al.* [12] described a two-stage program for DAM transition with a *Trem2*-independent step (stage 1) where *Tyrobp* and other genes are upregulated, followed by a *Trem2*-dependent step during which both *Tyrobp* and *Trem2* are upregulated (stage 2). Krasemann *et al.*[20] described a very similar microglial signature associated with neurodegenerative diseases, designated the “MGnD” phenotype, and showed that the transition from homeostatic to MGnD microglia was both TREM2- and apolipoprotein E (APOE)-dependent with a TREM2-APOE signaling pathway driving the transition from homeostatic microglia to MGnD. *APOE* $\epsilon$ 4, one of the *APOE* polymorphisms, is a major risk factor for late-onset AD, and emerging evidence suggests that APOE (mostly produced by astrocytes in a normal brain) can also bind to TREM2 [21,22]. This event defines an interesting and potentially disease-relevant pathway wherein extracellular APOE, as a ligand for TREM2, triggers upregulation of APOE in microglia.

When DAM and MGnD are compared, Keren-Shaul *et al.*[12] also observed by single-cell RNA sequencing an apparent sequence of events whereby *Tyrobp* was upregulated prior to the upregulation of *Trem2*. For clarity, since DAM and MGnD microglia appear to share key features of the phenomena described here, we will refer only to DAM for the remainder of this report. However, insofar as we are aware, principles established here underpin both DAM and MGnD.

In light of the central role of TYROBP in the microglial sensome[10], its key role as adaptor for multiple microglial receptors[23], its upregulation in the early *Trem2*-independent DAM stage 1[12] and its upregulation in AD[11], we hypothesized that the upregulation of *Tyrobp* might be an early event that begins during the initial microglial response to the accumulation of A $\beta$  deposits. Further, we propose that chronic sustained sensation of A $\beta$  deposits by microglia might generate ongoing intracellular signals that influence the progression and pathogenesis of AD.

## 1.2 Study design and main results

We employed a number of strategies aimed at interrogation of the causes and consequences of *TYROBP* upregulation in microglia. Using dual RNA *in situ* hybridization and immunohistochemistry, we found that *Tyrobp* mRNA level is significantly increased when microglia are recruited, including in wild-type (WT) mice, in an *APP/PSEN1* transgenic mouse model of cerebral A $\beta$  amyloidosis, and in a *MAPT<sup>P301S</sup>* transgenic mouse model of tauopathy. To determine whether elevated TYROBP can modify microglial phenotype and AD pathogenesis, we generated a novel transgenic mouse, designated the *Iba1<sup>Tyrobp</sup>* mouse, wherein the *Iba1* promoter was used to drive overexpression of a mouse *Tyrobp* transgene in microglia. We observed a reduced density of amyloid plaques and an apparent increase in the stoichiometry of TAU phosphorylation when *Iba1<sup>Tyrobp</sup>* mice were crossed with either *APP/PSEN1* or *MAPT<sup>P301S</sup>* mice, respectively. In addition to the alteration of both *APP/PSEN1* and *MAPT<sup>P301S</sup>* phenotypes, we observed that a constitutive increase in TYROBP

influenced the transcription of *ApoE* and some associated genes. Finally, using two mouse models of cerebral A $\beta$  amyloidosis and a mouse model of penetrating cortical stab injury, we showed that upregulation of *Tyrobp* and *ApoE* does not require *Trem2*, but that upregulation of microglial *ApoE* requires *Tyrobp* to reach normal levels.

### 1.3 Trem2-Tyrobp-ApoE choreography

*TREM2*, *TYROBP* and *APOE* are three microglial genes linked in a pathway contributing to the pathogenesis of AD and in the transition to DAM[12]. *TYROBP* was identified as a key driver in sporadic late-onset AD[11]. *TREM2* binds to *TYROBP*, its intracellular adaptor, to initiate its signal transduction pathway, and naturally occurring loss-of-function mutations of either *TYROBP* or *TREM2* can lead to Nasu-Hakola disease[15,24]. There is a general assumption among investigators in this research area that genetic deletion or overexpression of either *TREM2* or *TYROBP* would result in identical phenotypes in disease models, but, until now, this has not been tested directly. We previously demonstrated amelioration of behavioral and electrophysiological deficits in *APP/PSEN1* and *MAPT<sup>P301S</sup>* mice on a *Tyrobp*-null background, despite a concurrent absence of effect on amyloid pathology and an apparent increase in the stoichiometry of phosphorylated TAU vs total TAU[25–27]. Homozygous deletion of *Trem2* can also lead to amelioration of both amyloidosis and tauopathy [28,29], but those effects vary according to the mouse model, and the age and level of deficiency at sacrifice [27,30,31]. Lee *et al.*[32] used bacterial artificial chromosome (BAC)-mediated transgenesis to overexpress the human *TREM2* in the mouse genome and showed that *TREM2* overexpression reduces amyloid accumulation in 5xFAD mice. Using a similar BAC system, Gratuze *et al.*[33] assessed the impact of *TREM2<sup>R47H</sup>* in *MAPT<sup>P301S</sup>* mice but no *TREM2* overexpression was reported in that study.

The possible existence of an early *TREM2*-independent phase in conversion of microglia to DAM was described by Keren-Shaul *et al.*[12] but was not evident in studies by either Krasemann *et al.*[20] or Zhou *et al.*[34] *ApoE* has also been described as a participant in stage 1 of DAM with *Tyrobp*[12], and it has been suggested that *APOE* drives the DAM transition through a *TREM2*-*APOE* pathway[20]. Moreover, *ApoE* has been reported to influence both amyloidosis and tauopathy histological phenotypes in mouse models[35,36]. A complete elucidation of the choreography of the regulatory interactions among these genes and their cognate proteins therefore remains an area of intense interest. We would suggest that the discrepancies across the various analyses might be explained in part by the fact that DAM microglia are located in the immediate proximity of the plaques, and that neither bulk- nor single-cell- RNA sequencing can distinguish homeostatic vs DAM phenotypes since both techniques generate an average transcriptomic analysis from all microglia within a particular tissue sample. This formulation played a major role in prompting us to use dual RNA *in situ* hybridization and immunohistochemistry in the current study in which we sought to determine 1) the effects of transgenic overexpression of *Tyrobp* on amyloid and tau pathologies and 2) the relationship of the induction of *Tyrobp* to these pathologies and to the induction of *Trem2* and *ApoE*.

While this manuscript was in preparation, Chen *et al.* (2020)[37] reported spatial transcriptomics and *in situ* sequencing in *App<sup>NL-G-F</sup>* mice, employing this protocol due to

considerations identical to those motivating our studies herein; i.e., in order to avoid any potential confound derived from averaging the transcriptomes in a tissue sample without providing for spatial resolution of isolated resident microglia vs plaque-associated recruited microglia. These investigators proposed the formulation of a plaque-induced gene (PIG) network within the microglia and astrocytes in immediate proximity to amyloid plaques; this PIG network was defined by differential expression of 57 genes[37]. Top genes highly upregulated in the proximity of the plaques and as early as 3 months of age were *Tyrobp*, *ApoE* and several complement-related genes. Notably, *Tyrobp* is a key regulator of the complement subnetwork[11], and C1q is down-regulated in *APP/PSEN1* and *MAPT<sup>P301S</sup>* mice in the absence of *Tyrobp*[26,27]. The authors performed the same type of experiment in human AD brain slices and confirmed the enrichment of *Tyrobp* and several complement components (*C1qA*, *C1qB*, *C1qC*, and *Clu*). Of particular relevance to our data herein, *Trem2* was not included in the human PIG network.

#### 1.4 Study conclusions and perspectives

In addition to confirming that TYROBP overexpression in microglia is sufficient to alter both amyloidosis and tauopathy phenotypes, our data indicate that *Tyrobp* upregulation is an early marker of recruited microglia and can occur even in the brains of *Trem2*-deficient mice. Similarly, we observed that the increased *ApoE* mRNA level in microglia is *Trem2*-independent, whether in injury or AD-related mouse models. Finally, we observed that microglial *ApoE* mRNA level was greatly attenuated in plaque-associated microglia in *Tyrobp*-deficient mice. These data confirm the model proposed by Keren-Shaul *et al.*[12] in which *Tyrobp* and *ApoE* transcripts are increased first, and neither transcription event requires the presence of *Trem2*. Moreover, Meilandt *et al.*[38] recently reported that microglial APOE expression was not reduced, but, on the contrary, was increased in *PS2APP;Trem2<sup>-/-</sup>* mice when compared with microglial APOE expression in *PS2APP;Trem2<sup>+/+</sup>* mice. In that same study, Meilandt and colleagues also analyzed the expression profiles of FACS-purified microglia from *5xFAD* mice that expressed TREM2 normally and from FACS-purified microglia from *5xFAD* mice deficient in *Trem2*. These investigators observed a two-fold reduction in *ApoE* in one dataset (GSE132508)[12,38] but no reduction at all in the other (GSE65067)[38,39]. However, Parhizkar *et al.*[40] reported that the absence of functional TREM2 reduces plaque-associated APOE. This is in line with what Krasemann *et al.*[20] proposed when they showed that genetic targeting of *Trem2* suppresses the APOE pathway. Our observations and conclusions herein apparently differ from those of Parhizkar *et al.*[40] to the extent that, in our hands, microglial amyloid plaque sensing followed by upregulation of *Tyrobp* and *ApoE* are preserved in the absence of *Trem2* and, as a consequence of the *Trem2* deficiency, microglia recruitment into the proximity of amyloid plaques is reduced. This relationship points to the fact that the absence of functional TREM2 will block appearance of the full DAM phenotype and therefore the associated clearance of A $\beta$  is reduced. Nevertheless, we propose a model wherein the sensing of amyloid plaques -- which takes place upstream of amyloid plaque clearance-- involves *Tyrobp* and *ApoE* but not necessarily *Trem2*. Since APOE isoforms differentially influence AD age at onset and progression[41], future investigations will be aimed at elucidating whether and how various homozygous or heterozygous APOE isotype combinations affect TYROBP-APOE signaling, and/or microglial sensing and phenotyping switching[42].

TYROBP is a 113 amino acid polypeptide with a minimal extracellular region[43,44], making it unlikely that TYROBP is the sole player in a signal transduction pathway involving both the perception of the environment and the triggering of the switch from homeostatic phenotype to DAM. However, TYROBP is the adaptor for many receptors other than TREM2[23], and therefore, it is plausible and perhaps likely that other TYROBP receptors could play key roles in sensing the deposition of amyloid. For example, numerous SIGLEC proteins (sialic acid-binding immunoglobulin-type lectins) carry a positively charged residue in their transmembrane domain that participates in oligomerization of the SIGLEC with TYROBP. The primary SIGLEC ligand is a sialic acid that accumulates in many pathological conditions including cerebral A $\beta$  amyloidosis[45,46]. Moreover, Siglec-H interacts with TYROBP, and its expression has been reported to be elevated in *5xFAD* mice[32]. CD33 (SIGLEC-3) is also one of the most abundant SIGLECs in human brain, and genome-wide association studies (GWAS) implicated a polymorphism near *CD33* as a genetic risk factor for AD[2,4,47]. CD33 and TREM2 both interact with TYROBP, either directly (TREM2) or via common intracellular signaling factors (CD33). Griciuc *et al.*[48] recently investigated crosstalk between CD33 and TREM2 and proposed that CD33 acts upstream of TREM2. They also showed that *Cd33* and *Tyrobp* expression levels did not change in *Trem2*<sup>-/-</sup> versus WT microglia. This formulation provides evidence that CD33-TYROBP signaling could occur upstream of the recruitment and upregulation of TREM2.

Rather than the somewhat exclusively “*Trem2*-centric” view of DAM proposed in the existing AD microglia literature[20,34,40], we propose that *Tyrobp* can play a central role in an alternative and early pathway in the microglial sensome[10], even in the absence of any change in *Trem2* levels. The data that we present here document the robust consequences of TYROBP overexpression in both *APP/PSEN1* and *MAPT*<sup>P301S</sup> mice. We confirm here that upregulation in microglia of both *Tyrobp* and *ApoE* constitute interconnected events in microglia sensing of amyloid deposits, and that these events take place independently of *Trem2*.

## 2. CONSOLIDATED RESULTS AND STUDY DESIGN

With the inclusion of *Tyrobp* as a PIG gene[37] and because of our prior validation of its actions as a driver of AD[11,25–27], we hypothesized that constitutive overexpression of microglial *Tyrobp* via transgenesis would alter both amyloid and tau pathologies. In 4-month-old *APP/PSEN1* mice, *Tyrobp* overexpression was associated with a 50% decreased in the amyloid burden, similar to what occurs with the upregulation of *Trem2*[32] (Fig. 3A–B). We confirmed this decrease by measuring levels of human A $\beta$ 42 and A $\beta$ 40 by ELISA in the cerebral cortices of these mice (Fig. 3C). An evaluation of plaque burden in 8-month-old mice in three different brain regions confirmed the magnitude and statistical significance associated with the reduction of amyloid burden (Fig. 3G–H). In *MAPT*<sup>P301S</sup> mice, we previously reported that deficiency of *Tyrobp* increased TAU phosphorylation and spread[27], and we were puzzled, therefore, to observe a similar increase in TAU phosphorylation in the *MAPT*<sup>P301S</sup> mice with overexpression of *Tyrobp* (Fig. 4A–C). *MAPT*<sup>P301S</sup>; *Iba1*<sup>Tyrobp</sup> microglia are also more reactive compared to *MAPT*<sup>P301S</sup> microglia, and reactive microglia have been reported to drive TAU pathology, so these two observations are compatible (Fig. 4D–E, Supp Fig. 2B)[49,50]. This exacerbation of pathology under

conditions of either down- or up-regulation of *Tyrobp* in *MAPT<sup>P301S</sup>* mice reveals the complexity of the microglial events underpinning tauopathy. Our formulation is that, for any particular microglial activation status, there exists some optimum level of *Tyrobp* expression, and that either elevation or deficiency of *Tyrobp* levels can be detrimental. These data also support a key role for microglial TYROBP in AD pathology progression, as we proposed in our previous reports on mice deficient in *Tyrobp*[25–27].

Despite the obvious differences across *APP/PSEN1* and *MAPT<sup>P301S</sup>* mouse models and the diverse consequences of *Tyrobp* upregulation in each of these mice, there are shared changes in *Axl*, *Ccl2*, *Tgfb* and *Il6* mRNAs in both *APP/PSEN1* or *MAPT<sup>P301S</sup>* mice overexpressing TYROBP (Fig. 3F and 4F). These genes have been recently associated with *ApoE* in microglia, macrophages, and mononuclear phagocytes. AXL has been identified as a regulator of APOE[51], and accumulation of IL6 and CCL2 have been associated with APOE overexpression[52,53]. Similarly, reciprocal suppression of TGFβ and induction of APOE have been described in DAM microglia[20]. *ApoE* mRNA levels are indeed upregulated in *MAPT<sup>P301S</sup>;Iba1<sup>Tyrobp</sup>* mice as compared to *MAPT<sup>P301S</sup>* mice, but *ApoE* levels are unchanged in *APP/PSEN1;Iba1<sup>Tyrobp</sup>* mice as compared to *APP/PSEN1* mice (Fig. 3F and 4F). However, in bulk RNA sequencing performed on hippocampi from male *APP/PSEN1;Iba1<sup>Tyrobp</sup>* vs *APP/PSEN1* mice, we identified *ApoE* as a potential (activation z-score: 2.44; p-value overlap: 0.224) upstream regulator (Supp Fig. 3), suggesting the possible existence of a relationship between *Tyrobp* upregulation and *ApoE*. While a TREM2-APOE pathway has been described[20], it is interesting to note that our data indicate that the TYROBP-APOE relationship is detectable even in the absence of *Trem2* upregulation (Fig. 3F and 4F).

To investigate further the interactions among *Trem2*, *Tyrobp* and *ApoE* in microglia, we used a penetrating cortical stab injury paradigm by introducing a small lesion via stereotactic surgery into one hemisphere of the mouse brain in order to induce a recruitment of microglia around the injury site<sup>32</sup>. Using this experimental paradigm in WT, *Trem2<sup>-/-</sup>* or *Tyrobp<sup>-/-</sup>* mice, we confirmed that microglia upregulate both *Tyrobp* mRNA and *ApoE* mRNA when recruited in close proximity to the injury (Fig. 5A–D), and these events are readily detectable even in the absence of *Trem2*. Interestingly, we failed to observe an upregulation of *ApoE* mRNA in microglia from *Tyrobp<sup>-/-</sup>* mice subjected to penetrating cortical stab injury (Fig. 5C). Because microglia are also recruited around Aβ plaques, we used two different mouse models of human cerebral Aβ-amyloidosis (i.e., *TgCRND8* and *APP/PSEN1* mouse lines) that were either WT or gene-targeted for *Trem2* or *Tyrobp*, respectively. Similarly, we observed that both *Tyrobp* and *ApoE* mRNAs were upregulated in amyloid plaque-associated microglia even in the absence of *Trem2* (Fig. 6A–B). Moreover, and as predicted with the stab-injury paradigm, we observed a substantial decrease in the induction of *ApoE* mRNA in plaque-associated microglia when *Tyrobp* was absent (Fig. 6D).

### 3. DETAILED METHODS AND RESULTS

#### 3.1 Methods

See Supplementary Methods

## 3.2 Results

**3.2.1 *Tyrobp* transcription is increased in recruited microglia**—Microglia continuously sense changes in the brain environment and are recruited to sites of injury, microbial invasion, or where abnormal folding or modification of cellular constituents are detected, as with the accumulation of aggregated A $\beta$ . We performed dual RNA *in situ* hybridization (RNAscope®) and immunohistochemistry for *Tyrobp* and IBA1 respectively in WT mice and observed increased levels of *Tyrobp* mRNA in areas exhibiting recruited microglia (Fig 1A). Using the same experimental approach in two independent mouse models of cerebral amyloidosis (*APP/PSEN1*[54] and *5xFAD*[55]), we observed a similar pattern in that the *Tyrobp* mRNA level was extensively and selectively increased in microglia recruited in close proximity to amyloid plaques as compared to microglia that are more distant from the plaques (Fig. 1B–C). We similarly assayed *Tyrobp* mRNA and IBA1 protein in the *MAPT<sup>P301S</sup>* mice[56] (also known as PS19), a mutant tauopathy mouse model. We previously described an elevated number of anti-phosphorylated-TAU immunostained neurons in the piriform cortex of this mouse model (Fig. 1D)[27]. The changes that we observed in these mice were analogous to the changes observed around amyloid plaques in that we detected increased amounts of *Tyrobp* mRNA in microglia surrounding areas of aggregated protein pathology (Fig. 1D). We confirmed the increase of TYROBP at the protein level in microglia around amyloid plaques (Fig. 1E) as previously reported[57]. To discriminate between the role of TYROBP in activated vs recruited microglia, we isolated primary microglia from WT mice and exposed them to the gram-negative bacterial endotoxin lipopolysaccharide (LPS) to induce microglial activation[58], the status of which we established by quantifying the robust increase of *Tnfa* mRNA following LPS treatment. Interestingly, *Tyrobp* mRNA level was unchanged, suggesting that *Tyrobp* transcription may be increased only when microglia are *both* recruited *and* activated but not in resident microglia despite evidence that these residents are also activated (Fig. 1F).

**3.2.2 Microglia are normal in *Iba1<sup>Tyrobp</sup>* mice**—To determine whether constitutive elevation of TYROBP via transgenesis may influence microglial phenotype and progression of AD pathology, we generated a novel transgenic mouse overexpressing *Tyrobp* selectively in microglia in the central nervous system. We used the mouse *Tyrobp* and *Enhanced Green Fluorescent Protein* (EGFP) sequences separated by an Internal Ribosome Entry Site (IRES) under the control of the mouse *Iba1* regulatory sequences (Supp Fig. 1 [59]). Microinjections were performed in C57BL/6J mice and one line (B6.Cg-Tg(*Iba1-Tyrobp*-IRES-*Egfp*)34Mee/J) was selected for further use based on expression level of the transgene, now referred to *Iba1<sup>Tyrobp</sup>*. We first assessed the overexpression of *Tyrobp* mRNA by RT-qPCR and measured a  $\approx$  2.5-fold increase (Fig. 2A). Despite this elevated mRNA level, western blot analyses of protein extracts from the cortex did not reveal a significant overexpression at the protein level (Fig. 2B). Using combined RNA *in situ* hybridization and immunohistochemistry for *Tyrobp* and IBA1, respectively, in mice deficient in TYROBP (*Tyrobp*<sup>-/-</sup>), WT or overexpressing *Tyrobp* on the *Iba1* promoter (*Iba1<sup>Tyrobp</sup>*), we confirmed the 2-fold increase in *Tyrobp* mRNA in *Iba1<sup>Tyrobp</sup>* mice compared to WT (Fig. 2C–D). We observed that only a subset of microglia was overexpressing *Tyrobp* mRNA in *Iba1<sup>Tyrobp</sup>* mice. This selectivity is likely due to the use of the *Iba1* promoter in a WT background



without extensive microglia activation, thereby also accounting for the lack of a significant increase of TYROBP at the protein level in the resting state. RNA sequencing of hippocampi from *Iba1<sup>Tyrobp</sup>* mice did not reveal any differentially expressed genes (DEGs) other than *Aif1* (= *Iba1*), which is increased due to the inclusion of the first two exons in the transgenic vector (Supp Fig. 1). These data indicate that *Iba1<sup>Tyrobp</sup>* microglia do not display molecular and phenotypic changes in mice that are lacking in certain backgrounds of aggregated protein pathology.

### 3.2.3 TYROBP overexpression in microglia decreases amyloid plaque load in *APP/PSEN1* mice

—To assess whether TYROBP overexpression in microglia modulates A $\beta$  deposition in *APP/PSEN1* mice, double-heterozygous *APP/PSEN1;Iba1<sup>Tyrobp</sup>* mice were generated and studied at 4 months of age. We measured a  $\approx$ 50% decrease of the plaque density in the cerebral cortices of both male and female *APP/PSEN1;Iba1<sup>Tyrobp</sup>* mice compared to sex-matched *APP/PSEN1* mice (Fig. 3A–B) in sections stained for amyloid plaques using Thioflavin S (ThioS). This observation was supported by measuring levels of human A $\beta$ 42 and A $\beta$ 40 by ELISA, both of which were apparently associated with a trend toward decreases in the cortex with TYROBP overexpression, mostly among male *APP/PSEN1;Iba1<sup>Tyrobp</sup>* mice (Fig. 3C). There was no genotype-dependent difference in the number of plaque-associated microglia (Fig. 3D–E), unlike what has been reported in *5xFAD* mice in the presence of a transgenic increase in TREM2[32]. To evaluate microglial activation, we probed both groups with anti-IBA1 antibody and observed a weaker staining in *APP/PSEN1;Iba1<sup>Tyrobp</sup>* mice (Supp Fig. 2A). We next performed RT-qPCR on a group of microglial genes previously described in homeostatic or activated microglia. There was a significant increase of *Axl* and *Ccl2* and a decrease of *Cd68* and *Tgfb $\beta$*  in brains of *APP/PSEN1;Iba1<sup>Tyrobp</sup>* mice (Fig. 3F). Finally, we observed that the decrease of amyloid plaques persisted in 8-month-old *APP/PSEN1;Iba1<sup>Tyrobp</sup>* mice as shown by the decreased percentage of ThioS positive areas in somatomotor, hippocampus, and visual areas (Fig. 3G–H).

### 3.2.4 TYROBP overexpression in *MAPT<sup>P301S</sup>* mice increases TAU phosphorylation and microglial activation

—We previously reported that deletion of *Tyrobp* altered both mouse amyloidosis and tauopathy phenotypes and the microglial response to these pathologies[25–27]. In *MAPT<sup>P301S</sup>;Iba1<sup>Tyrobp</sup>* double heterozygous mice, western blot analyses using AT8 and T205 antibodies revealed increased levels of phosphorylated-TAU (pTAU) in the cortex of both male and female mice compared to *MAPT<sup>P301S</sup>* mice at 4 months of age, whereas total human TAU levels detected with the HT7 antibody were unchanged (Fig. 4A–B). Increased pTAU within brains from *MAPT<sup>P301S</sup>;Iba1<sup>Tyrobp</sup>* mice was further confirmed immunohistochemically (Fig. 4C). We also observed increased IBA1 intensity in *MAPT<sup>P301S</sup>;Iba1<sup>Tyrobp</sup>* compared to *MAPT<sup>P301S</sup>* mice and this IBA1 increase was correlated with the increased pTAU (Fig. 4D, Supp Fig. 2B). We confirmed an increased microglial activation state by double-label immunohistochemistry with anti-IBA1 and anti-CD68 in the piriform cortex (Fig. 4E). Using RT-qPCR, we measured increases of *Tyrobp*, *P2ry12*, *ApoE*, *Axl*, *Itgax*, *Iba1*, *Tgfb $\beta$*  and *Il6* mRNAs in *MAPT<sup>P301S</sup>;Iba1<sup>Tyrobp</sup>* mice compared to *MAPT<sup>P301S</sup>* mice (Fig. 4F).

**3.2.5 Induction of microglial *Tyrobp* and *ApoE* is *Trem2*-independent in a model of cortical stab injury**—To assess the interactions amongst *Trem2*, *Tyrobp* and *ApoE* in microglia, we used an injury paradigm by introducing a small penetrating cortical stab injury via stereotactic surgery into one hemisphere of the mouse brain in order to induce a recruitment of microglia around the injury site[60]. We first used injured- WT mice and combined RNA *in situ* hybridization and immunohistochemistry for *ApoE* and IBA1 respectively. In the intact hemisphere, most *ApoE* mRNA was not located in microglia but rather in astrocytes, the source of most APOE in brain. However, *ApoE* mRNA was dramatically increased in microglia recruited on the lesioned side (Fig. 5A–B). Following the same procedure in *Tyrobp*<sup>-/-</sup> mice, *ApoE* mRNA was not induced in microglia on either side (Fig. 5C), but strikingly, mRNA levels of *Tyrobp* and *ApoE* were highly upregulated in the recruited microglia of injured *Trem2*<sup>-/-</sup> mice (Fig. 5D, Supp Fig. 4). Taken together, these data indicate that *Tyrobp* upregulation in recruited microglia around the traumatic lesion is *Trem2*-independent. Moreover, the increase of *ApoE* transcripts in recruited microglia in the same mouse model of injury appears to be *Tyrobp*-dependent but *Trem2*-independent.

**3.2.6 Induction of microglial *Tyrobp* and *ApoE* around amyloid plaques is *Trem2*-independent, and *ApoE* upregulation is dramatically decreased when *Tyrobp* is absent**—In order to investigate further these interactions among *Trem2*, *Tyrobp* and *ApoE* in microglia in the presence of mutant human *APP*, we first performed dual RNA *in situ* hybridization and immunohistochemistry for *Tyrobp*, IBA1 and 6E10 in *TgCRND8* mice[61] on either a WT or *Trem2*-null background. Despite reduced recruitment of microglia around plaques when *Trem2* was deleted[57], *Tyrobp* mRNA was still increased in plaque-associated microglia (Fig. 6A) as was *ApoE* mRNA in plaque-associated microglia in the same *TgCRND8*; *Trem2*<sup>-/-</sup> mice (Fig. 6B). We confirmed that the plaques-associated microglia upregulating *Tyrobp* were the ones upregulating *ApoE* (Fig. 6C). We then assayed *APP/PSEN1* mice that were either WT or deficient in *Tyrobp* and, while the expression of *ApoE* was not completely abolished by deletion of *Tyrobp*, we confirmed a substantial decrease in the induction of *ApoE* mRNA in plaque-associated microglia when *Tyrobp* was absent (Fig. 6D).

In summary, our results provide compelling evidence that: 1) upregulation of *Tyrobp* mRNA level is an early event occurring in recruited microglia; 2) TYROBP-APOE signaling in the microglial sensome is readily detectable even in the absence of *Trem2*. We propose that activation of the TYROBP-APOE pathway could be an early or even initiating step in the transformation of microglia from the homeostatic phenotype to the DAM phenotype (Figure 7).

## Supplementary Material

Refer to Web version on PubMed Central for supplementary material.

## ACKNOWLEDGEMENTS

The study was supported by the National Institute on Aging (U01 AG046170 and R01 AG057907 to MEE, SG and BZ), the Alzheimer's Disease Research Division of the BrightFocus Foundation (grant A2018253F to MA and

grant A2016482F to JVHM), the Mount Sinai Alzheimer's Disease Research Center (ADRC P50 AG005138 and P30 AG066514 to Mary Sano, with internal pilot grant awarded to MA). Figure 7 was created with [BioRender.com](https://BioRender.com).

## REFERENCES

- [1]. Lambert JC, Ibrahim-Verbaas CA, Harold D, Naj AC, Sims R, Bellenguez C, et al. Meta-analysis of 74,046 individuals identifies 11 new susceptibility loci for Alzheimer's disease. *Nat Genet* 2013;45:1452–8. 10.1038/ng.2802. [PubMed: 24162737]
- [2]. Naj AC, Jun G, Beecham GW, Wang L-S, Vardarajan BN, Buross J, et al. Common variants at MS4A4/MS4A6E, CD2AP, CD33 and EPHA1 are associated with late-onset Alzheimer's disease. *Nat Genet* 2011;43:436–41. 10.1038/ng.801. [PubMed: 21460841]
- [3]. Lambert J-C, Zelenika D, Hiltunen M, Chouraki V, Combarros O, Bullido MJ, et al. Evidence of the association of BIN1 and PICALM with the AD risk in contrasting European populations. *Neurobiol Aging* 2011;32:756.e11–15. 10.1016/j.neurobiolaging.2010.11.022.
- [4]. Hollingworth P, Harold D, Sims R, Gerrish A, Lambert J-C, Carrasquillo MM, et al. Common variants at ABCA7, MS4A6A/MS4A4E, EPHA1, CD33 and CD2AP are associated with Alzheimer's disease. *Nat Genet* 2011;43:429–35. 10.1038/ng.803. [PubMed: 21460840]
- [5]. Jun G, Naj AC, Beecham GW, Wang L-S, Buross J, Gallins PJ, et al. Meta-analysis confirms CR1, CLU, and PICALM as Alzheimer disease risk loci and reveals interactions with APOE genotypes. *Arch Neurol* 2010;67:1473–84. 10.1001/archneurol.2010.201. [PubMed: 20697030]
- [6]. Lambert J-C, Heath S, Even G, Campion D, Sleegers K, Hiltunen M, et al. Genome-wide association study identifies variants at CLU and CR1 associated with Alzheimer's disease. *Nat Genet* 2009;41:1094–9. 10.1038/ng.439. [PubMed: 19734903]
- [7]. Harold D, Abraham R, Hollingworth P, Sims R, Gerrish A, Hamshere ML, et al. Genome-wide association study identifies variants at CLU and PICALM associated with Alzheimer's disease. *Nat Genet* 2009;41:1088–93. 10.1038/ng.440. [PubMed: 19734902]
- [8]. Jansen IE, Savage JE, Watanabe K, Bryois J, Williams DM, Steinberg S, et al. Genome-wide meta-analysis identifies new loci and functional pathways influencing Alzheimer's disease risk. *Nat Genet* 2019;51:404–13. 10.1038/s41588-018-0311-9. [PubMed: 30617256]
- [9]. Kunkle BW, Grenier-Boley B, Sims R, Bis JC, Damotte V, Naj AC, et al. Genetic meta-analysis of diagnosed Alzheimer's disease identifies new risk loci and implicates A $\beta$ , tau, immunity and lipid processing. *Nat Genet* 2019;51:414–30. 10.1038/s41588-019-0358-2. [PubMed: 30820047]
- [10]. Hickman SE, Kingery ND, Ohsumi TK, Borowsky ML, Wang L, Means TK, et al. The microglial sensome revealed by direct RNA sequencing. *Nat Neurosci* 2013;16:1896–905. 10.1038/nn.3554. [PubMed: 24162652]
- [11]. Zhang B, Gaiteri C, Bodea L-G, Wang Z, McElwee J, Podtelezchnikov AA, et al. Integrated systems approach identifies genetic nodes and networks in late-onset Alzheimer's disease. *Cell* 2013;153:707–20. 10.1016/j.cell.2013.03.030. [PubMed: 23622250]
- [12]. Keren-Shaul H, Spinrad A, Weiner A, Matcovitch-Natan O, Dvir-Szternfeld R, Ulland TK, et al. A Unique Microglia Type Associated with Restricting Development of Alzheimer's Disease. *Cell* 2017;169:1276–1290.e17. 10.1016/j.cell.2017.05.018.
- [13]. Guerreiro R, Wojtas A, Bras J, Carrasquillo M, Rogaeva E, Majounie E, et al. TREM2 variants in Alzheimer's disease. *N Engl J Med* 2013;368:117–27. 10.1056/NEJMoa1211851. [PubMed: 23150934]
- [14]. Zhou S-L, Tan C-C, Hou X-H, Cao X-P, Tan L, Yu J-T. TREM2 Variants and Neurodegenerative Diseases: A Systematic Review and Meta-Analysis. *JAD* 2019;68:1171–84. 10.3233/JAD-181038. [PubMed: 30883352]
- [15]. Paloneva J, Kestilä M, Wu J, Salminen A, Böhring T, Ruotsalainen V, et al. Loss-of-function mutations in TYROBP (DAPI2) result in a presenile dementia with bone cysts. *Nat Genet* 2000;25:357–61. 10.1038/77153. [PubMed: 10888890]
- [16]. Pottier C, Ravenscroft TA, Brown PH, Finch NA, Baker M, Parsons M, et al. TYROBP genetic variants in early-onset Alzheimer's disease. *Neurobiol Aging* 2016;48:222.e9–222.e15. 10.1016/j.neurobiolaging.2016.07.028.

- [17]. Zhao Y, Wu X, Li X, Jiang L-L, Gui X, Liu Y, et al. TREM2 Is a Receptor for  $\beta$ -Amyloid that Mediates Microglial Function. *Neuron* 2018;97:1023–1031.e7. 10.1016/j.neuron.2018.01.031.
- [18]. Hansen DV, Hanson JE, Sheng M. Microglia in Alzheimer's disease. *The Journal of Cell Biology* 2018;217:459–72. 10.1083/jcb.201709069. [PubMed: 29196460]
- [19]. Montalvo V, Quigley L, Vistica BP, Boelte KC, Nugent LF, Takai T, et al. Environmental factors determine DAP12 deficiency to either enhance or suppress immunopathogenic processes. *Immunology* 2013;140:475–82. 10.1111/imm.12158. [PubMed: 23906311]
- [20]. Krasemann S, Madore C, Cialic R, Baufeld C, Calcagno N, El Fatimy R, et al. The TREM2-APOE Pathway Drives the Transcriptional Phenotype of Dysfunctional Microglia in Neurodegenerative Diseases. *Immunity* 2017;47:566–581.e9. 10.1016/j.immuni.2017.08.008. [PubMed: 28930663]
- [21]. Mahley RW. Apolipoprotein E: Remarkable Protein Sheds Light on Cardiovascular and Neurological Diseases. *Clin Chem* 2017;63:14–20. 10.1373/clinchem.2016.255695. [PubMed: 28062606]
- [22]. Mahley RW, Weisgraber KH, Huang Y. Apolipoprotein E4: a causative factor and therapeutic target in neuropathology, including Alzheimer's disease. *Proc Natl Acad Sci U S A* 2006;103:5644–51. 10.1073/pnas.0600549103. [PubMed: 16567625]
- [23]. Lanier LL. DAP10- and DAP12-associated receptors in innate immunity. *Immunological Reviews* 2009;227:150–60. 10.1111/j.1600-065X.2008.00720.x. [PubMed: 19120482]
- [24]. Dardiotis E, Siokas V, Pantazi E, Dardioti M, Rikos D, Xiromerisiou G, et al. A novel mutation in TREM2 gene causing Nasu-Hakola disease and review of the literature. *Neurobiology of Aging* 2017;53:194.e13–194.e22. 10.1016/j.neurobiolaging.2017.01.015.
- [25]. Haure-Mirande J-V, Audrain M, Fanutza T, Kim SH, Klein WL, Glabe C, et al. Deficiency of TYROBP, an adapter protein for TREM2 and CR3 receptors, is neuroprotective in a mouse model of early Alzheimer's pathology. *Acta Neuropathol* 2017;134:769–88. 10.1007/s00401-017-1737-3. [PubMed: 28612290]
- [26]. Haure-Mirande J-V, Wang M, Audrain M, Fanutza T, Kim SH, Heja S, et al. Integrative approach to sporadic Alzheimer's disease: deficiency of TYROBP in cerebral A $\beta$  amyloidosis mouse normalizes clinical phenotype and complement subnetwork molecular pathology without reducing A $\beta$  burden. *Mol Psychiatry* 2018. 10.1038/s41380-018-0255-6.
- [27]. Audrain M, Haure-Mirande J-V, Wang M, Kim SH, Fanutza T, Chakrabarty P, et al. Integrative approach to sporadic Alzheimer's disease: deficiency of TYROBP in a tauopathy mouse model reduces C1q and normalizes clinical phenotype while increasing spread and state of phosphorylation of tau. *Mol Psychiatry* 2018. 10.1038/s41380-018-0258-3.
- [28]. Jay TR, Miller CM, Cheng PJ, Graham LC, Bemiller S, Broihier ML, et al. TREM2 deficiency eliminates TREM2+ inflammatory macrophages and ameliorates pathology in Alzheimer's disease mouse models. *The Journal of Experimental Medicine* 2015;212:287–95. 10.1084/jem.20142322. [PubMed: 25732305]
- [29]. Leyns CEG, Ulrich JD, Finn MB, Stewart FR, Koscal LJ, Remolina Serrano J, et al. TREM2 deficiency attenuates neuroinflammation and protects against neurodegeneration in a mouse model of tauopathy. *Proc Natl Acad Sci USA* 2017;114:11524–9. 10.1073/pnas.1710311114. [PubMed: 29073081]
- [30]. Bemiller SM, McCray TJ, Allan K, Formica SV, Xu G, Wilson G, et al. TREM2 deficiency exacerbates tau pathology through dysregulated kinase signaling in a mouse model of tauopathy. *Mol Neurodegener* 2017;12:74. 10.1186/s13024-017-0216-6. [PubMed: 29037207]
- [31]. Sayed FA, Telpoukhovskaia M, Kodama L, Li Y, Zhou Y, Le D, et al. Differential effects of partial and complete loss of TREM2 on microglial injury response and tauopathy. *Proc Natl Acad Sci USA* 2018;115:10172–7. 10.1073/pnas.1811411115. [PubMed: 30232263]
- [32]. Lee CYD, Daggett A, Gu X, Jiang L-L, Langfelder P, Li X, et al. Elevated TREM2 Gene Dosage Reprograms Microglia Responsivity and Ameliorates Pathological Phenotypes in Alzheimer's Disease Models. *Neuron* 2018;97:1032–1048.e5. 10.1016/j.neuron.2018.02.002.
- [33]. Gratzke M, Leyns CEG, Sauerbeck AD, St-Pierre M-K, Xiong M, Kim N, et al. Impact of TREM2R47H variant on tau pathology-induced gliosis and neurodegeneration. *Journal of Clinical Investigation* 2020;10.1172/JCI138179. 10.1172/JCI138179.

- [34]. Zhou Y, Song WM, Andhey PS, Swain A, Levy T, Miller KR, et al. Human and mouse single-nucleus transcriptomics reveal TREM2-dependent and TREM2-independent cellular responses in Alzheimer's disease. *Nat Med* 2020;26:131–42. 10.1038/s41591-019-0695-9. [PubMed: 31932797]
- [35]. Shi Y, Manis M, Long J, Wang K, Sullivan PM, Remolina Serrano J, et al. Microglia drive APOE-dependent neurodegeneration in a tauopathy mouse model. *J Exp Med* 2019. 10.1084/jem.20190980.
- [36]. Ulrich JD, Ulland TK, Mahan TE, Nyström S, Nilsson KP, Song WM, et al. ApoE facilitates the microglial response to amyloid plaque pathology. *J Exp Med* 2018;215:1047–58. 10.1084/jem.20171265. [PubMed: 29483128]
- [37]. Chen W-T, Lu A, Craessaerts K, Pavie B, Sala Frigerio C, Corthout N, et al. Spatial Transcriptomics and In Situ Sequencing to Study Alzheimer's Disease. *Cell* 2020:S0092867420308151. 10.1016/j.cell.2020.06.038.
- [38]. Meilandt WJ, Ngu H, Gogineni A, Lalehzadeh G, Lee S-H, Srinivasan K, et al. Trem2 deletion reduces late-stage amyloid plaque accumulation, elevates the A $\beta$ 42:A $\beta$ 40 ratio, and exacerbates axonal dystrophy and dendritic spine loss in the PS2APP Alzheimer's mouse model. *J Neurosci* 2020:1871–19. 10.1523/JNEUROSCI.1871-19.2019.
- [39]. Wang Y, Cella M, Mallinson K, Ulrich JD, Young KL, Robinette ML, et al. TREM2 lipid sensing sustains the microglial response in an Alzheimer's disease model. *Cell* 2015;160:1061–71. 10.1016/j.cell.2015.01.049. [PubMed: 25728668]
- [40]. Parhizkar S, Arzberger T, Brendel M, Kleinberger G, Deussing M, Focke C, et al. Loss of TREM2 function increases amyloid seeding but reduces plaque-associated ApoE. *Nature Neuroscience* 2019. 10.1038/s41593-018-0296-9.
- [41]. Kloske CM, Wilcock DM. The Important Interface Between Apolipoprotein E and Neuroinflammation in Alzheimer's Disease. *Front Immunol* 2020;11:754. 10.3389/fimmu.2020.00754. [PubMed: 32425941]
- [42]. Fitz NF, Wolfe CM, Playso BE, Biedrzycki RJ, Lu Y, Nam KN, et al. Trem2 deficiency differentially affects phenotype and transcriptome of human APOE3 and APOE4 mice. *Mol Neurodegeneration* 2020;15:41. 10.1186/s13024-020-g00394-4.
- [43]. Lanier LL, Corliss BC, Wu J, Leong C, Phillips JH. Immunoreceptor DAP12 bearing a tyrosine-based activation motif is involved in activating NK cells. *Nature* 1998;391:703–7. 10.1038/35642. [PubMed: 9490415]
- [44]. Tomasello E, Olcese L, Vély F, Georgeon C, Bléry M, Moqrach A, et al. Gene structure, expression pattern, and biological activity of mouse killer cell activating receptor-associated protein (KARAP)/DAP-12. *J Biol Chem* 1998;273:34115–9. 10.1074/jbc.273.51.34115. [PubMed: 9852069]
- [45]. Siddiqui SS, Matar R, Merheb M, Hodeify R, Vazhappilly CG, Marton J, et al. Siglecs in Brain Function and Neurological Disorders. *Cells* 2019;8. 10.3390/cells8101125.
- [46]. Salminen A, Kaamiranta K. Siglec receptors and hiding plaques in Alzheimer's disease. *J Mol Med* 2009;87:697–701. 10.1007/s00109-009-0472-1. [PubMed: 19390836]
- [47]. Bertram L, Lange C, Mullin K, Parkinson M, Hsiao M, Hogan MF, et al. Genome-wide association analysis reveals putative Alzheimer's disease susceptibility loci in addition to APOE. *Am J Hum Genet* 2008;83:623–32. 10.1016/j.ajhg.2008.10.008. [PubMed: 18976728]
- [48]. Griciuc A, Patel S, Federico AN, Choi SH, Innes BJ, Oram MK, et al. TREM2 Acts Downstream of CD33 in Modulating Microglial Pathology in Alzheimer's Disease. *Neuron* 2019;103:820–835.e7. 10.1016/j.neuron.2019.06.010. [PubMed: 31301936]
- [49]. Maphis N, Xu G, Kokiko-Cochran ON, Jiang S, Cardona A, Ransohoff RM, et al. Reactive microglia drive tau pathology and contribute to the spreading of pathological tau in the brain. *Brain* 2015;138:1738–55. 10.1093/brain/awv081. [PubMed: 25833819]
- [50]. Asai H, Ikezu S, Tsunoda S, Medalla M, Luebke J, Haydar T, et al. Depletion of microglia and inhibition of exosome synthesis halt tau propagation. *Nat Neurosci* 2015;18:1584–93. 10.1038/nn.4132. [PubMed: 26436904]
- [51]. Zhao W, Fan J, Kulic I, Koh C, Clark A, Mueller J, et al. Axl receptor tyrosine kinase is a regulator of apolipoprotein E. *Mol Brain* 2020;13:66. 10.1186/s13041-020-00609-1.

- [52]. Levy O, Lavalette S, Hu SJ, Housset M, Raoul W, Eandi C, et al. APOE Isoforms Control Pathogenic Subretinal Inflammation in Age-Related Macular Degeneration. *J Neurosci* 2015;35:13568–76. 10.1523/JNEUROSCI.2468-15.2015. [PubMed: 26446211]
- [53]. Levy O, Calippe B, Lavalette S, Hu SJ, Raoul W, Dominguez E, et al. Apolipoprotein E promotes subretinal mononuclear phagocyte survival and chronic inflammation in age-related macular degeneration. *EMBO Mol Med* 2015;7:211–26. 10.15252/emmm.201404524. [PubMed: 25604058]
- [54]. Jankowsky JL, Fadale DJ, Anderson J, Xu GM, Gonzales V, Jenkins NA, et al. Mutant presenilins specifically elevate the levels of the 42 residue beta-amyloid peptide in vivo: evidence for augmentation of a 42-specific gamma secretase. *Hum Mol Genet* 2004;13:159–70. 10.1093/hmg/ddh019. [PubMed: 14645205]
- [55]. Oakley H, Cole SL, Logan S, Maus E, Shao P, Craft J, et al. Intraneuronal beta-amyloid aggregates, neurodegeneration, and neuron loss in transgenic mice with five familial Alzheimer's disease mutations: potential factors in amyloid plaque formation. *J Neurosci* 2006;26:10129–40. 10.1523/JNEUROSCI.1202-06.2006. [PubMed: 17021169]
- [56]. Yoshiyama Y, Higuchi M, Zhang B, Huang S-M, Iwata N, Saido TC, et al. Synapse loss and microglial activation precede tangles in a P301S tauopathy mouse model. *Neuron* 2007;53:337–51. 10.1016/j.neuron.2007.01.010. [PubMed: 17270732]
- [57]. Yuan P, Condello C, Keene CD, Wang Y, Bird TD, Paul SM, et al. TREM2 Haplodeficiency in Mice and Humans Impairs the Microglia Barrier Function Leading to Decreased Amyloid Compaction and Severe Axonal Dystrophy. *Neuron* 2016;90:724–39. 10.1016/j.neuron.2016.05.003. [PubMed: 27196974]
- [58]. Hoogland ICM, Houbolt C, van Westerlo DJ, van Gool WA, van de Beek D. Systemic inflammation and microglial activation: systematic review of animal experiments. *J Neuroinflammation* 2015;12:114. 10.1186/s12974-015-0332-6. [PubMed: 26048578]
- [59]. Tanaka KF, Matsui K, Sasaki T, Sano H, Sugio S, Fan K, et al. Expanding the Repertoire of Optogenetically Targeted Cells with an Enhanced Gene Expression System. *Cell Reports* 2012;2:397–406. 10.1016/j.celrep.2012.06.011. [PubMed: 22854021]
- [60]. Clarke D, Penrose MA, Harvey AR, Rodger J, Bates KA. Low intensity rTMS has sex-dependent effects on the local response of glia following a penetrating cortical stab injury. *Exp Neurol* 2017;295:233–42. 10.1016/j.expneurol.2017.06.019. [PubMed: 28624361]
- [61]. Chishti MA, Yang DS, Janus C, Phinney AL, Horne P, Pearson J, et al. Early-onset amyloid deposition and cognitive deficits in transgenic mice expressing a double mutant form of amyloid precursor protein 695. *J Biol Chem* 2001;276:21562–70. 10.1074/jbc.M100710200. [PubMed: 11279122]
- [62]. Kang SS, Kurti A, Baker KE, Liu C-C, Colonna M, Ulrich JD, et al. Behavioral and transcriptomic analysis of Trem2-null mice: not all knockout mice are created equal. *Human Molecular Genetics* 2018;27:211–23. 10.1093/hmg/ddx366. [PubMed: 29040522]
- [63]. Litvinchuk A, Wan Y-W, Swartzlander DB, Chen F, Cole A, Propson NE, et al. Complement C3aR Inactivation Attenuates Tau Pathology and Reverses an Immune Network Deregulated in Tauopathy Models and Alzheimer's Disease. *Neuron* 2018;100:1337–1353.e5. 10.1016/j.neuron.2018.10.031.

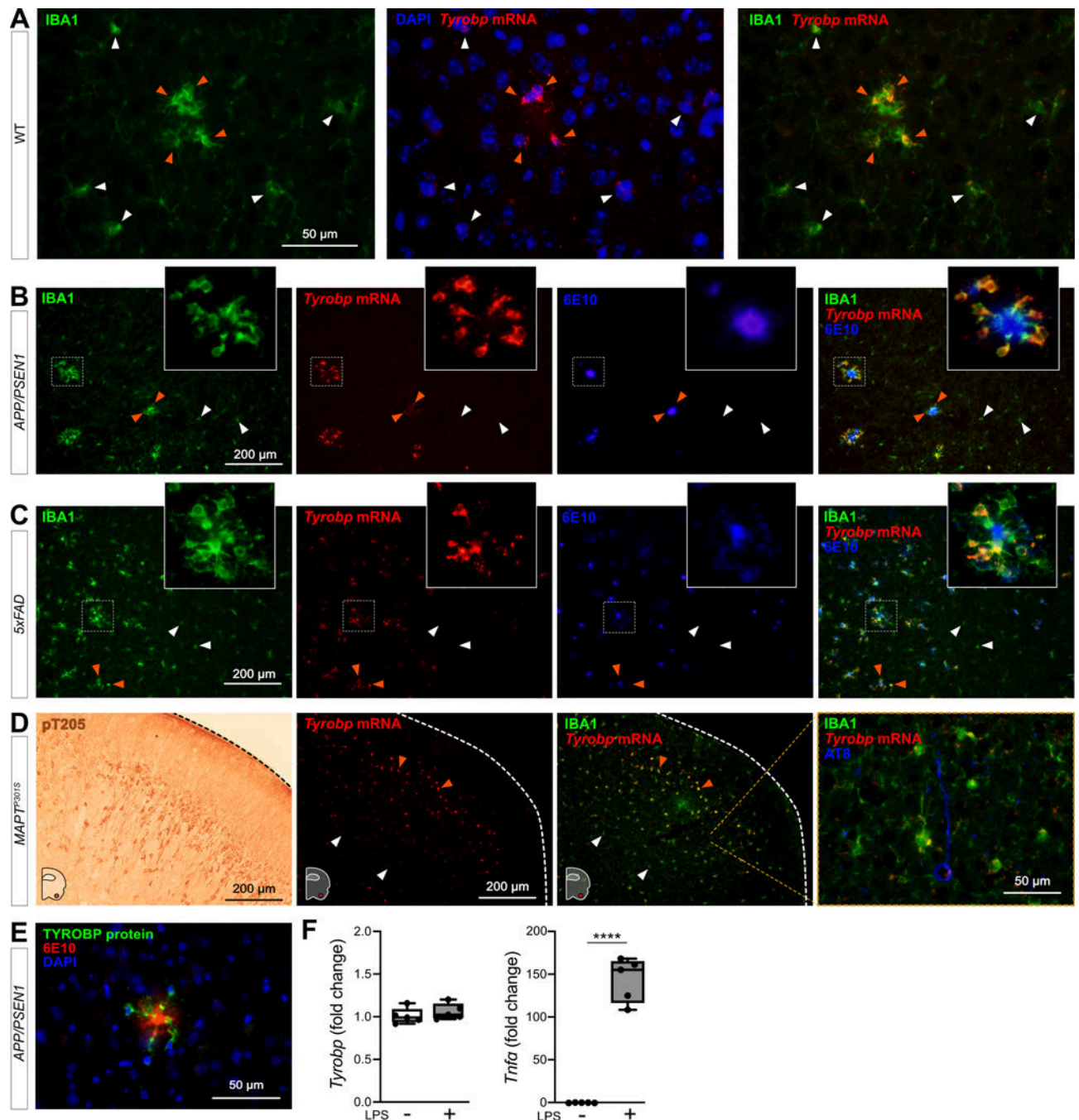


**Figure 1: *Tyrobp* mRNA is increased in recruited microglia**

(A) Dual RNA fluorescent *in situ* hybridization (RNAscope®) and immunohistochemistry for *Tyrobp* mRNA (red) and IBA1 protein (green) respectively in WT mice (DAPI in blue). Scale bar = 50  $\mu$ m. (B-C) Dual RNA *in situ* hybridization and immunohistochemistry for *Tyrobp* (red), IBA1 (Green) and A $\beta$  (antibody 6E10) (blue) in *APP/PSEN1* (B) and *5xFAD* (C) mice. Scale bar = 200  $\mu$ m. (D) Left panel: representative image of immunohistochemistry with antibody pT205 in the piriform cortex of *MAPT<sup>P301S</sup>* (PS19) mice. Scale bar = 200  $\mu$ m. Right panels: dual RNA *in situ* hybridization and

immunohistochemistry for *Tyrobp* (red), IBA1 (green) and pTau (antibody AT8) (blue) in the piriform cortex of *MAPT<sup>P301S</sup>* mice. Scale bars = 200 and 50  $\mu\text{m}$ . (E) Co-immunohistochemistry for TYROBP (green) and human A $\beta$  (antibody 6E10) (red) in *APP/PSEN1* mice (DAPI in blue). Scale bar = 50 $\mu\text{m}$ . (F) RT-qPCR analyses of *Tyrobp* and *TNF $\alpha$*  mRNAs in WT primary microglia with and without LPS. Mice were either 4 (A) or 8 (B-E) months of age and were all WT for *Tyrobp*. White and orange arrows indicate examples of non-recruited and recruited microglia, respectively. Slice thickness = 10 $\mu\text{m}$ .



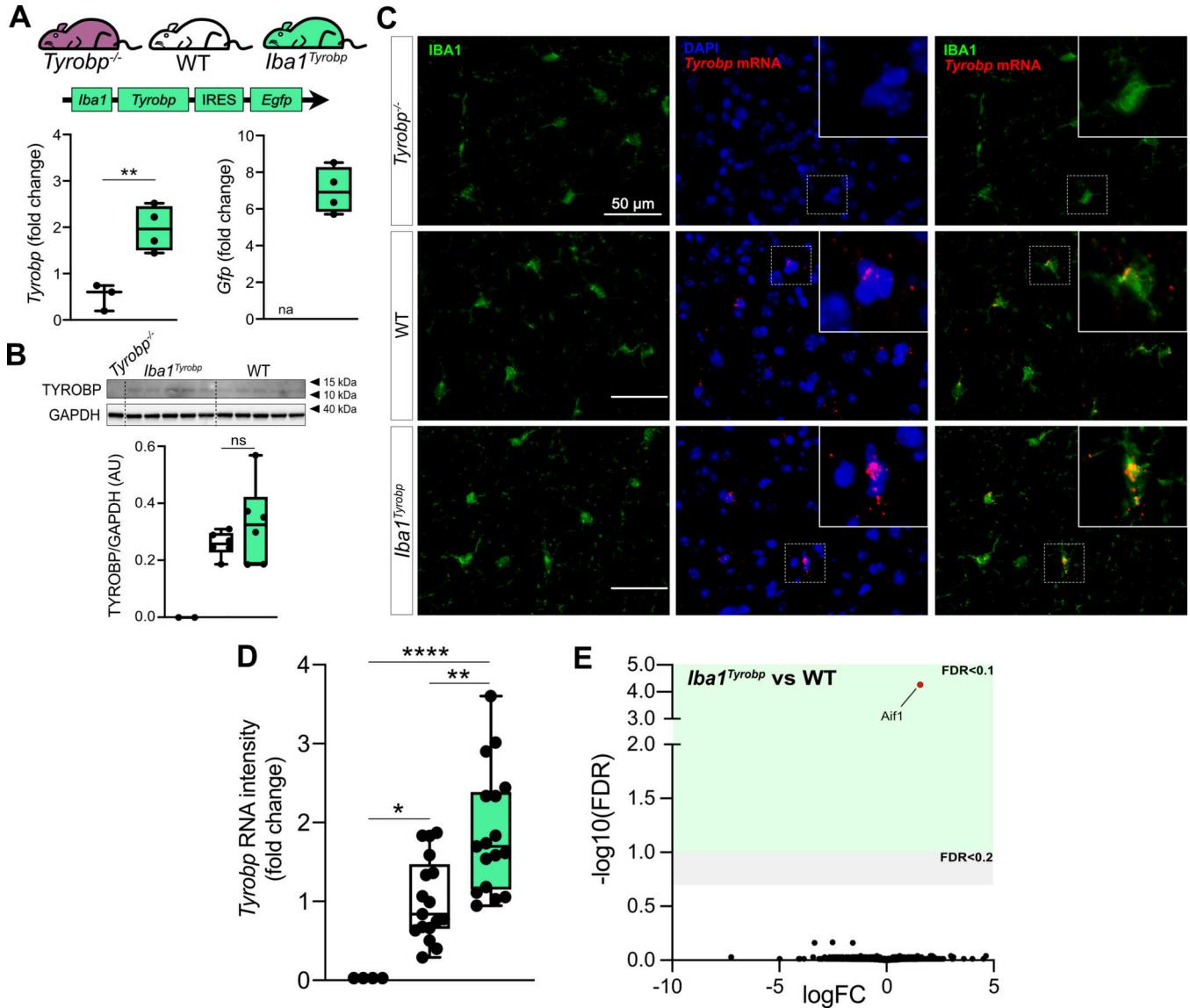


**Figure 2: Generation of *Iba1*<sup>Tyrobp</sup> mice**

(A) Hippocampi from 4-month old *Tyrobp*<sup>-/-</sup>, WT and *Iba1*<sup>Tyrobp</sup> mice were assayed for *Tyrobp* and *Gfp* mRNAs by RT-qPCR (n = 3–4 mice per group). (B) Representative western blot and quantification of TYROBP and GAPDH in the cortex of the same groups used in (A) (n = 2–6 mice per group). (C) Dual RNA fluorescent *in situ* hybridization and immunohistochemistry for *Tyrobp* mRNA (red) and IBA1 (green) respectively (DAPI in blue) in *Tyrobp*<sup>-/-</sup>, WT and *Iba1*<sup>Tyrobp</sup> mice. Scale bar = 50 μm and slice thickness = 10 μm. (D) Quantification of *Tyrobp* mRNA intensity from the experiment described in (C). n = 4, 17 and 17 slices per group (from N = 1 mouse per genotype) for *Tyrobp*<sup>-/-</sup>, WT and *Iba1*<sup>Tyrobp</sup> mice respectively. (E) Volcano plot representation of the whole hippocampal DEGs in *Iba1*<sup>Tyrobp</sup> vs WT mice (n = 4 4-month old males per genotype). Error bars represent means ± SEM. Statistical analyses were performed using a Student t-test (A) or a One-Way ANOVA followed by a Tukey’s post-hoc test (B, D), \*p < 0.05, \*\*p < 0.01, \*\*\*\*p < 0.0001. na = not applicable; ns = non-significant.

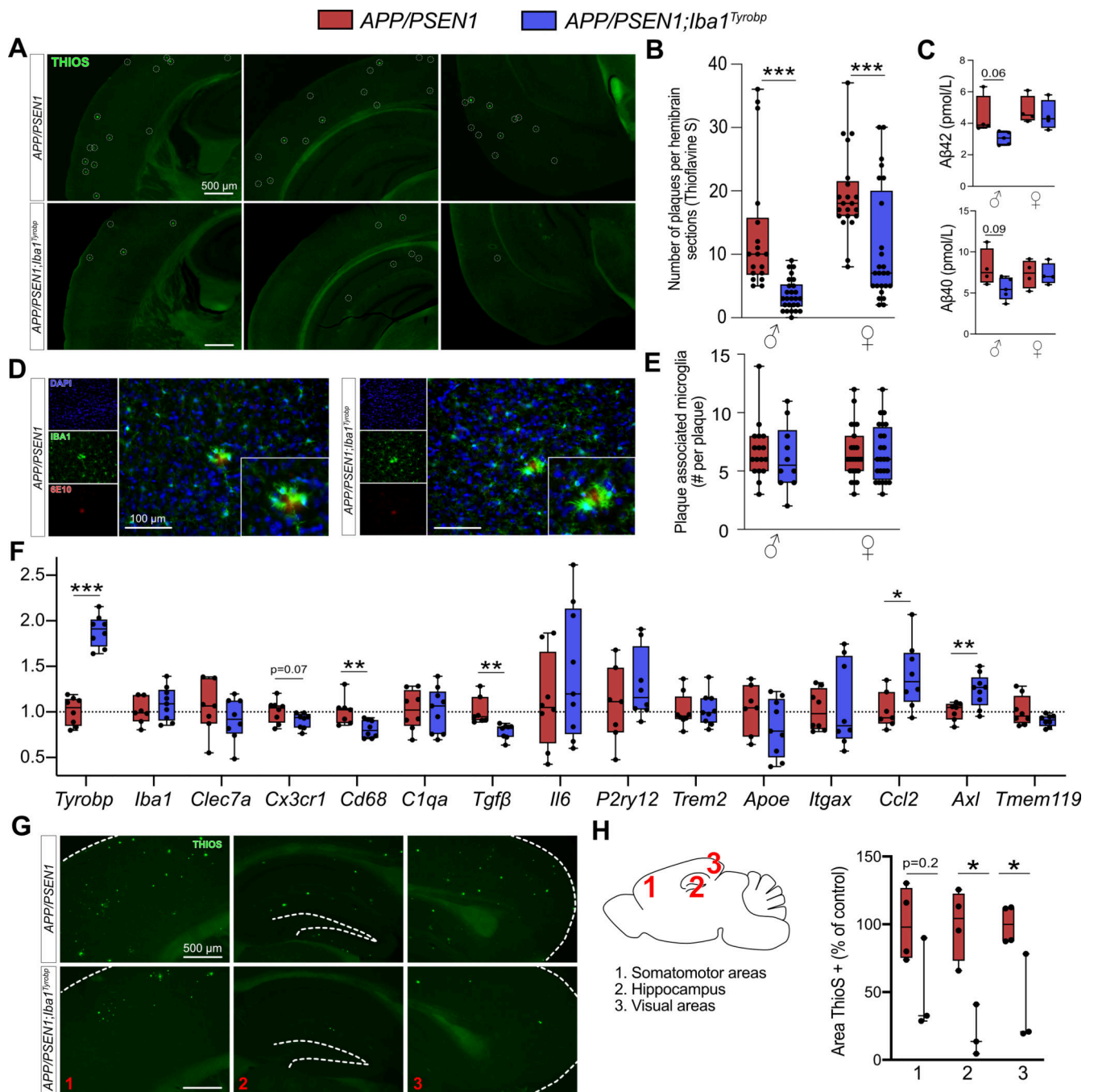


**Figure 3: Transgene-derived *Tyrobp* upregulation decreases amyloid plaque load in *APP/PSEN1* mice**

(A) Representative images of Thioflavine-S (ThioS) staining in *APP/PSEN1* and *APP/PSEN1;Iba1<sup>Tyrobp</sup>* mice at 4 months of age. Scale bar = 500  $\mu$ m. (B) Quantification of the number of ThioS-positive plaques per hemibrain in *APP/PSEN1* and *APP/PSEN1;Iba1<sup>Tyrobp</sup>* mice at 4 months of age. N = 4–5 mice per genotype and sex with 3 slices per animal. (C) Human A $\beta$ 42 and A $\beta$ 40 concentrations measured by ELISA in the cortices of the same groups described in (B). (D) Representative images of double-label immunohistochemistry with anti-IBA1 and anti-6E10 antibodies in *APP/PSEN1* and *APP/PSEN1;Iba1<sup>Tyrobp</sup>* mice at

4 months of age. Scale bar = 100  $\mu\text{m}$ . (E) Quantification of the number of plaque-associated microglia in the 4 groups described in (B). N = 10–24 plaques from 4–5 mice per group. (F) RT-qPCR analyses of microglial gene mRNAs in the hippocampi of *APP/PSEN1* and *APP/PSEN1;Iba1<sup>Tyrobp</sup>* mice at 4 months of age. N = 7–9 mice per group, females and males were pooled. (G) Representative images of ThioS staining in male *APP/PSEN1* and *APP/PSEN1;Iba1<sup>Tyrobp</sup>* mice at 8 months of age. Scale bar = 500  $\mu\text{m}$ . (H) Quantification of the ThioS immunoreactive area in male *APP/PSEN1* and *APP/PSEN1;Iba1<sup>Tyrobp</sup>* mice at 8 months of age (somatomotor and visual areas of the cortex, and hippocampus were quantified). N = 3–4 mice per group. Error bars represent means  $\pm$  SEM. Statistical analyses were performed using a Two-Way ANOVA followed by a Sidak post-hoc test for (B and E), a Kruskal-Wallis test for (C), a Student t-test for (F) and a Mann-Whitney test for (H), \* $p < 0.05$ , \*\* $p < 0.01$ , \*\*\* $p < 0.001$ .

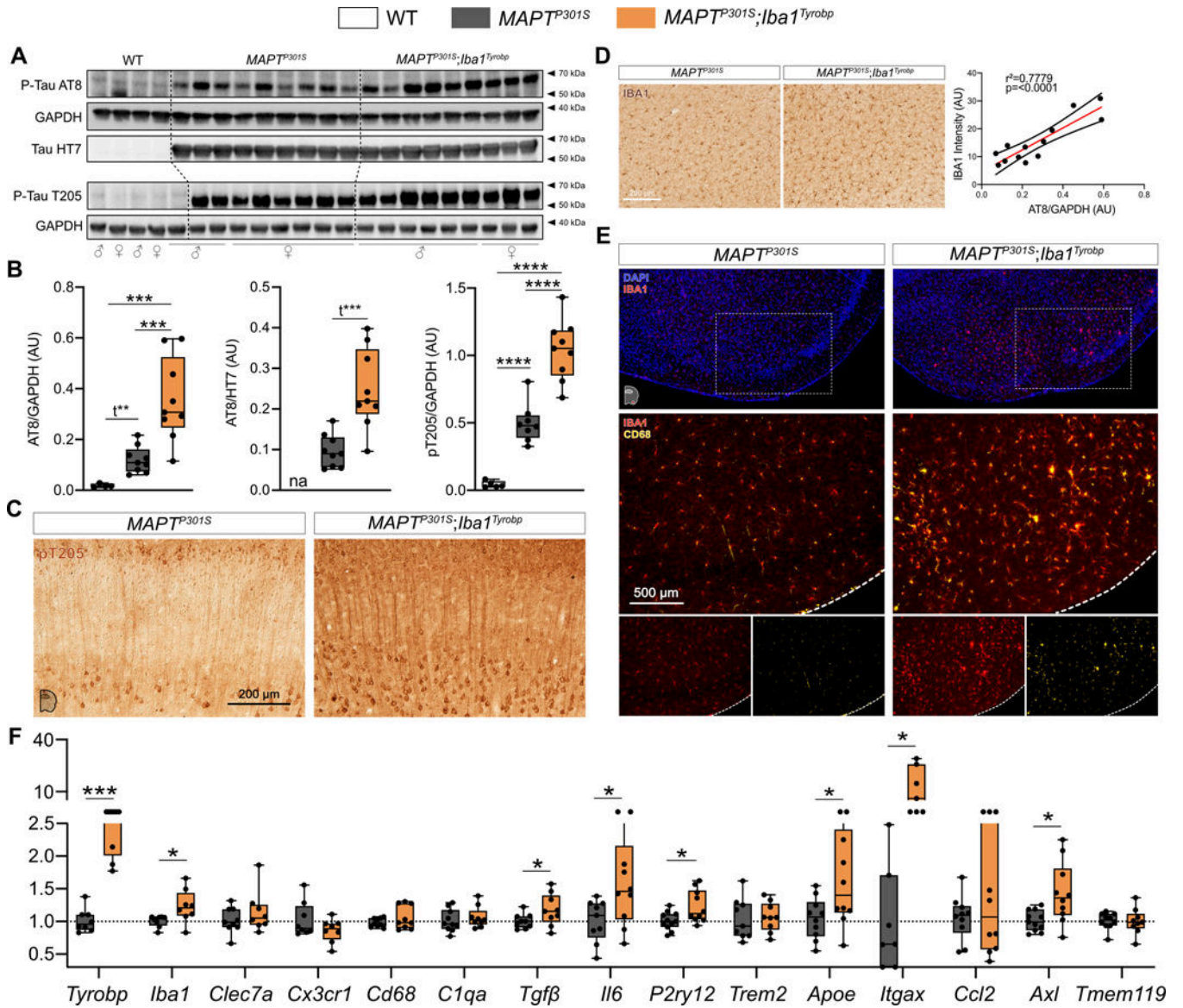


**Figure 4: Transgene-induced *Tyrobp* upregulation increases apparent stoichiometry of TAU phosphorylation and microglial activation in 4-month-old *MAPT<sup>P301S</sup>* mice**  
 (A) Western blot analyses of phosphorylated-TAU on S202 or T205 epitopes (AT8 and pT205 antibodies) and total human TAU (HT7 antibody) in cortical homogenates from WT, *MAPT<sup>P301S</sup>* (PS19) and *MAPT<sup>P301S</sup>;Iba1<sup>Tyrobp</sup>* mice at 4 months-old. n = 4–9 mice per group. (B) Densitometric analyses of western blots presented in (A) standardized to GAPDH or HT7. (C) Representative images of DAB-immunohistochemistry with antibody pT205 in 4 month-old *MAPT<sup>P301S</sup>* and *MAPT<sup>P301S</sup>;Iba1<sup>Tyrobp</sup>* mice. Scale bar = 200  $\mu$ m. (D) Left panel: representative images of anti-IBA1 immunohistochemistry on the same groups described in (C). Scale bar = 200  $\mu$ m. Additional representative pictures are presented in Supplementary Figure 2. Right panel: western blot-AT8/GAPDH quantification plotted against anti-IBA1 immunoreactivity in the cortex. Linear regression with trend line (red line) and 95% confidence intervals (black lines) are indicated. (E) Representative images of double-label immunofluorescence with anti-IBA1 and anti-CD68 antibodies in the piriform

cortex on the same groups described in (C). Scale bar = 500  $\mu\text{m}$ . (F) RT-qPCR analyses of microglial gene mRNAs in the hippocampus of *MAPT<sup>P301S</sup>* and *MAPT<sup>P301S</sup>;Iba1<sup>Tyrobp</sup>* mice at 4 months of age. N = 7–11 per group. Error bars represent means  $\pm$  SEM. Statistical analyses were performed using a One-Way ANOVA followed by a Tukey's post-hoc test for (B) or a Student t-test for (B) when \*t is indicated and (F), \*p<0.05, \*\*p<0.01, \*\*\*p<0.001, \*\*\*\*p<0.0001.

Author Manuscript

Author Manuscript

Author Manuscript

Author Manuscript

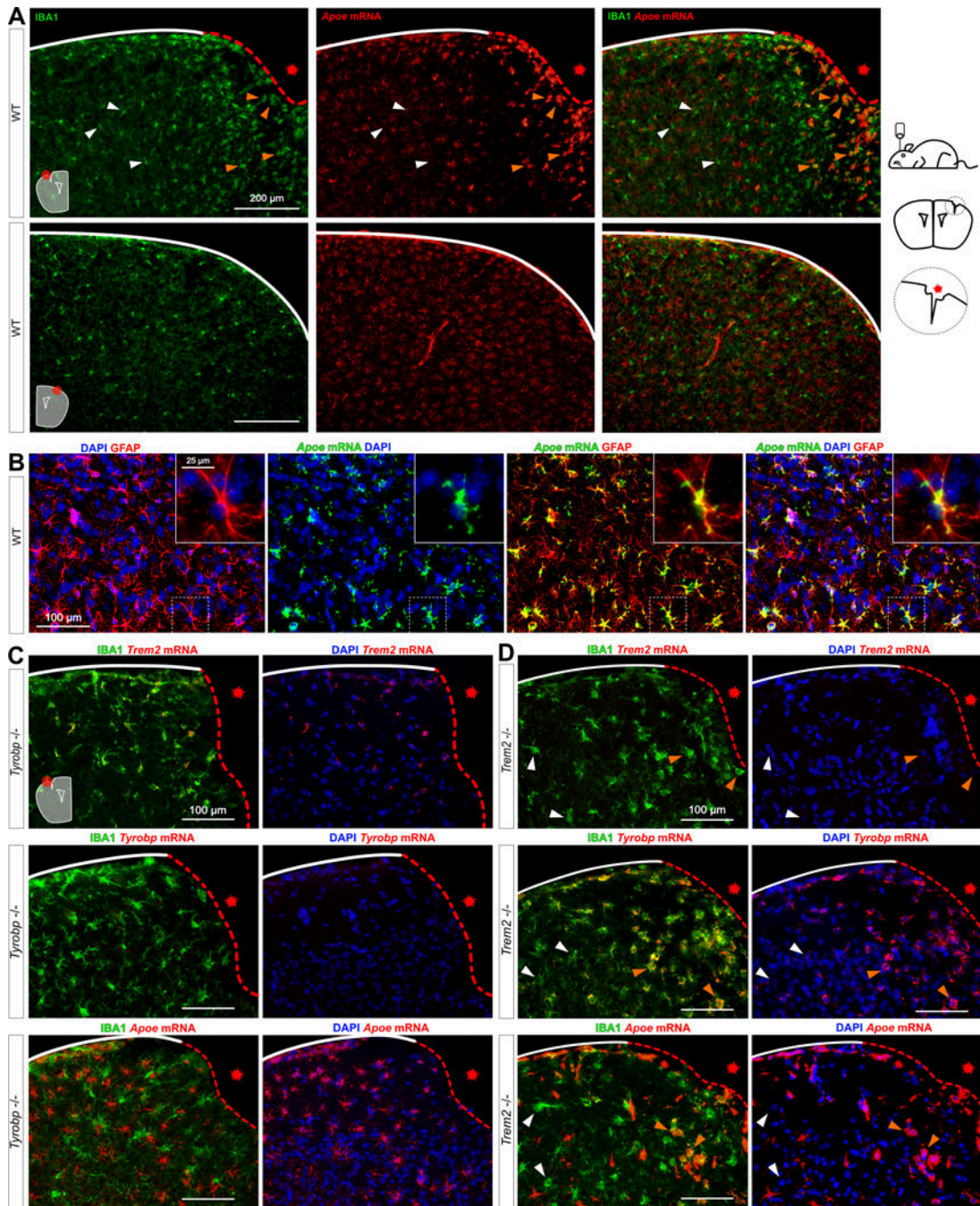


**Figure 5: Increases of *Tyrobp* and *Apoe* mRNAs in microglia recruited to a site of stab injury are *Trem2*-independent**

(A) Stab-injured WT mice were sacrificed 3 days after injury and dual RNA fluorescent *in situ* hybridization and immunohistochemistry for *Apoe* mRNA (red) and anti-IBA1 (green) respectively was performed. The injured ipsilateral area (red dotted line) is shown on the top row and the uninjured contralateral area is shown on the bottom row. Scale bar = 200 μm.

(B) Dual RNA fluorescent *in situ* hybridization and immunohistochemistry for *Apoe* (green) and GFAP (red) in non-injured WT mice. (C-D) The same stab injury protocol was utilized in *Tyrobp*<sup>-/-</sup> (C) and *Trem2*<sup>-/-</sup> (D) mice. Anti-IBA1 staining and DAPI staining are shown

in green and blue, respectively. Top row: *Trem2* mRNA (red); middle row: *Tyrbp* mRNA (red); bottom row: *ApoE* mRNA (red). Mice were 4 months of age, and slice thickness = 10  $\mu$ m. The red asterisk indicates the injured side. White and orange arrows indicate examples of non-recruited and recruited microglia, respectively.

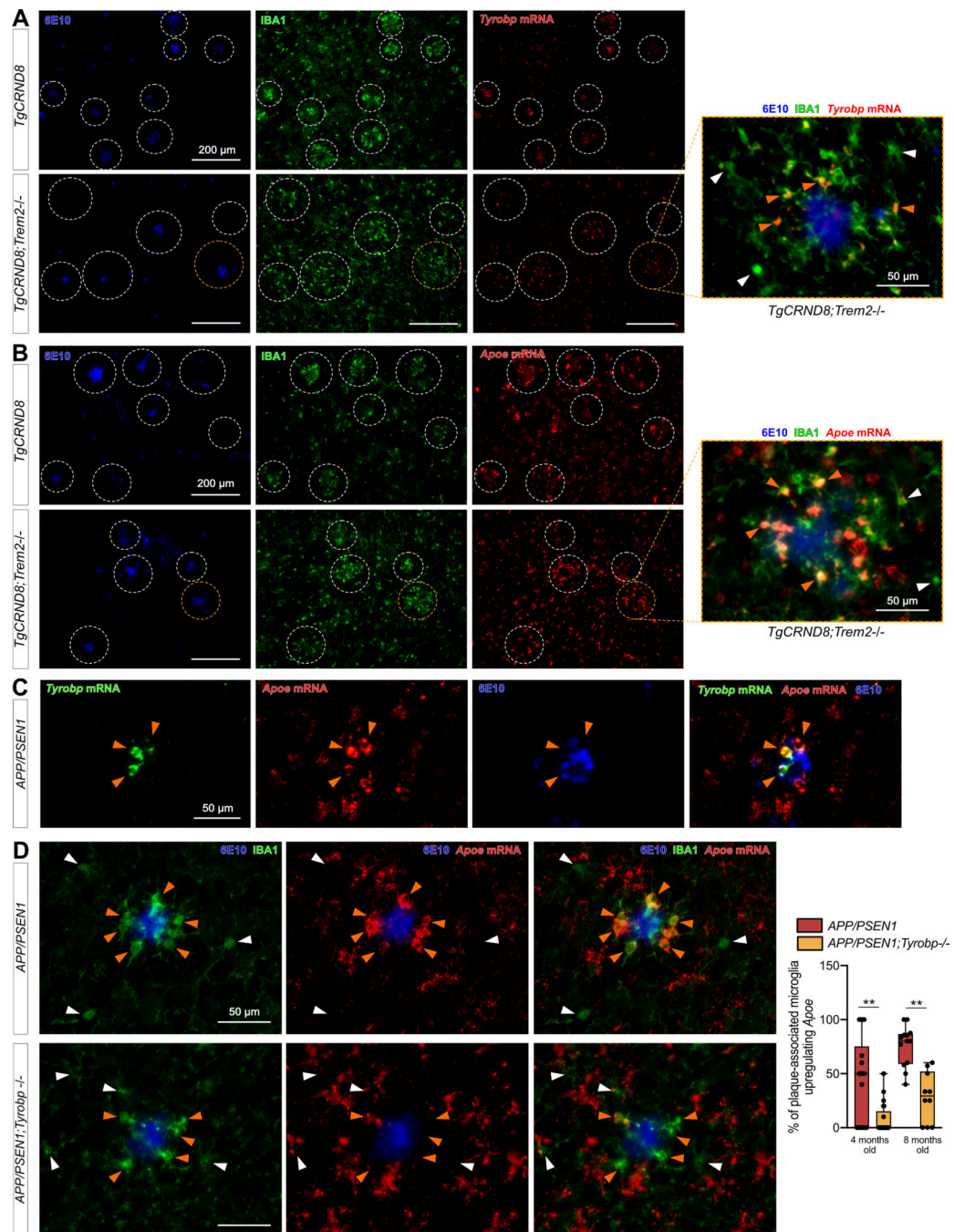


**Figure 6: Increases in *Tyrobp* and *Apoe* mRNAs in amyloid plaque-associated microglia are *Trem2* independent**

(A) Dual RNA fluorescent *in situ* hybridization and immunohistochemistry for *Tyrobp* mRNA (red), anti-IBA1 (green) and human A $\beta$  (6E10 antibody) (blue) in *TgCRND8* mice on WT (top row) or *Trem2*<sup>-/-</sup> (bottom row) background. Scale bar = 200 or 50  $\mu$ m. (B) Dual RNA fluorescent *in situ* hybridization and immunohistochemistry for *Apoe* mRNA (red), anti-IBA1 (green) and human amyloid (6E10 antibody) (blue) in the same mice as in (A). Scale bar = 200 or 50  $\mu$ m. (C) Dual RNA fluorescent *in situ* hybridization and immunohistochemistry for *Tyrobp* mRNA (green), *Apoe* mRNA (red) and 6E10 (blue) in APP/PSEN1 mice. (D) Dual RNA fluorescent *in situ* hybridization and immunohistochemistry for 6E10 (blue), IBA1 (green) and *Apoe* mRNA (red) in APP/PSEN1 mice. A bar graph shows the percentage of plaque-associated microglia upregulating *Apoe* in APP/PSEN1 (red bars) and APP/PSEN1; *Tyrobp*<sup>-/-</sup> (yellow bars) mice at 4 months old and 8 months old. Statistical significance is indicated by \*\*.



APP/PSEN1 mice. Scale bar = 50  $\mu$ m. (D) Dual RNA fluorescent *in situ* hybridization and immunohistochemistry for *ApoE* mRNA (red), anti-IBA1 (green) and human A $\beta$  (6E10 antibody) (blue) in *APP/PSEN1* mice on a WT (top row) or *Tyrobp*-null (bottom row) background. Scale bar = 50  $\mu$ m. Right panel: quantification of the number of plaque-associated microglia with upregulated *ApoE* mRNA in the same mice as in (D). N = 2–3 mice per group (A-D).

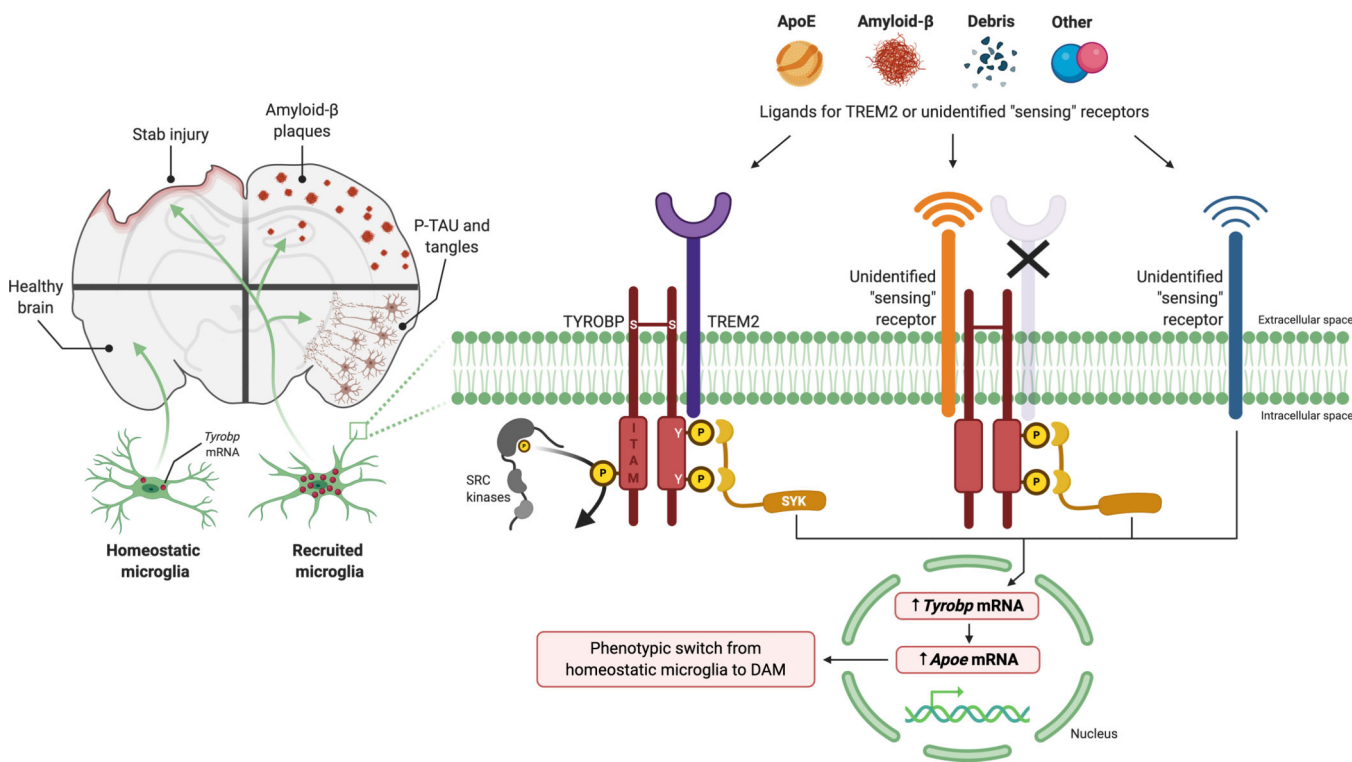


**Figure 7: Proposed ligand-induced Tyrobp signaling in recruited microglia**

Left panel: in response to penetrating stab injury or accumulation of amyloid- $\beta$  ( $A\beta$ ) deposits or misfolded tau, Tyrobp transcription is upregulated in microglia, thereby marking these cells as “recruited microglia”. Right panel: we observed that both microglial recruitment and Tyrobp upregulation occur in the absence of TREM2, indicating the existence of “sensing” receptors. Multiple alternative signaling pathways can be considered:

- Ligand signaling is initiated by apolipoprotein E,  $A\beta$ , debris, or other ligands at sensing receptors and leads to phosphorylation of the tyrosine residues in the cytoplasmic ITAM of TYROBP by SRC kinases and the recruitment of SYK. In turn, SYK signaling leads to up-regulated transcription of Tyrobp and ApoE. This series of events forms the basis for the phenotypic switch from homeostatic microglia to DAM.

- In mice lacking TREM2, microglial recruitment is retained, and transcription of both Tyrobp and ApoE is induced. Since these are constitutive TREM2 knockout mice, we are unable to exclude the possibility that some unknown sensor developed as compensation for the absence of TREM2. Another possibility is the existence of an unidentified sensing receptor that can upregulate TYROBP and APOE through a mechanism that does not require formation of TREM2/TYROBP complexes.

Abbreviations: TYROBP, tyrosine kinase binding protein; TREM2, triggering receptor expressed on myeloid cells-2; ITAM, immunoreceptor tyrosine-based activation motif; SYK, spleen tyrosine kinase; APOE, Apolipoprotein E; DAM, disease-associated microglia.